Title

Corridors of migrating neurons in the human brain and their decline during infancy.

Permalink

https://escholarship.org/uc/item/1rx9998w

Journal

Nature, 478(7369)

ISSN

0028-0836

Authors

Sanai, Nader
Nguyen, Thuhien
Ihrie, Rebecca A
et al.

Publication Date

2011-09-01

DOI

10.1038/nature10487

Peer reviewed

Published in final edited form as:
Nature. ; 478(7369): 382–386. doi:10.1038/nature10487.

Corridors of Migrating Neurons in Human Brain and Their Decline during Infancy

Nader Sanai[1,2,6], **Thuhien Nguyen**[1], **Rebecca A. Ihrie**[1], **Zaman Mirzadeh**[1,6], **Hui-Hsin Tsai**[1], **Michael Wong**[1], **Nalin Gupta**[2], **Mitchel S. Berger**[2], **Eric Huang**[3], **Jose-Manuel Garcia-Verdugo**[5], **David H. Rowitch**[1,2,4,7], and **Arturo Alvarez-Buylla**[1,2,7]

[1]Eli and Edythe Broad Institute of Regeneration Medicine and Stem Cell Research and Howard Hughes Medical Institute; University of California San Francisco, San Francisco, CA 94143

[2]Department of Neurological Surgery, University of California San Francisco, San Francisco, CA 94143

[3]Department of Pathology, University of California San Francisco, San Francisco, CA 94143

[4]Department of Pediatrics, University of California San Francisco, San Francisco, CA 94143

[5]Laboratorio de Morfología Celular, Unidad Mixta CIPF-UVEG, CIBERNED, Valencia 46012, Spain

[6]Barrow Brain Tumor Research Center, Barrow Neurological Institute, Phoenix, AZ, 85012

Abstract

The subventricular zone (SVZ) of many adult non-human mammals generates large numbers of new neurons destined for the olfactory bulb (OB)[1–6]. Along the walls of the lateral ventricles, immature neuronal progeny migrate in tangentially-oriented chains that coalesce into a rostral migratory stream (RMS) connecting the SVZ to the OB. The adult human SVZ, in contrast, contains a hypocellular gap layer separating the ependymal lining from a periventricular ribbon of astrocytes[7]. Some of these SVZ astrocytes can function as neural stem cells *in vitro*, but their function *in vivo* remains controversial. An initial report finds few SVZ proliferating cells and rare migrating immature neurons in the RMS of adult humans[7]. In contrast, a subsequent study indicates robust proliferation and migration in the human SVZ and RMS[8,9]. Here, we find that the infant human SVZ and RMS contain an extensive corridor of migrating immature neurons before 18 months of age, but, contrary to previous reports[8], this germinal activity subsides in older children and is nearly extinct by adulthood. Surprisingly, during this limited window of

---

[7] *Authors for correspondence:* Arturo Alvarez-Buylla and David H. Rowitch, Department of Neurological Surgery, University of California at San Francisco, 505 Parnassus Avenue, M779, Box 0112, San Francisco, CA 94143, abuylla@stemcell.ucsf.edu and rowitchd@peds.ucsf.edu.

Author Contributions

N.S. designed the study, acquired and interpreted experimental data, and prepared the manuscript. T.N. assisted with experiments, data collection and manuscript preparation. R.A.I. designed and conducted the EGFR experiments and assisted with manuscript preparation. Z.M. designed and conducted the whole-mount experiments. H.T. and M.W. conducted the *in situ* hybridization experiments. N.G., M.S.B, and E.H. assisted with specimen collection and neuropathological review. J.G. acquired and interpreted all ultrastructural analyses and assisted with study design. D.H.R. and A.A.B. designed the study, interpreted the data, and prepared the manuscript.

neurogenesis, not all new neurons in the human SVZ are destined for the OB – we describe a major migratory pathway that targets the prefrontal cortex in humans. Together, these findings reveal robust streams of tangentially migrating immature neurons in human early postnatal SVZ and cortex. These pathways represent potential targets of neurological injuries affecting neonates.

Keywords

human subventricular zone; rostral migratory stream; olfactory ventricle; medial migratory stream

We collected human brain specimens from 10 neurosurgical resections and 50 autopsied brains, ranging in age from birth to 84 years (Supp. Fig. 1; Supp. Table 1), using a protocol that allows subsequent analysis by fluorescent immunohistochemistry and *in situ* hybridization (see Methods). As shown (Fig. 1), staining of horizontal sections (30 μm) through the anterior horn of the lateral ventricle demonstrates that, in the first 6 months of life, the structure of the human SVZ in infants differs considerably from that observed in adults. The astrocytic ribbon and gap layer are not evident (Fig. 1) and, as seen in the fetal human brain[10,11], cells with elongated radial glial processes line the lateral ventricular wall that express vimentin and glial fibrillary acidic protein (GFAP)[11]. Adjacent to these radial glia, we observed a dense network of elongated unipolar and bipolar cells oriented tangentially to the ventricular lining. Many of these cells expressed the immature neuronal markers doublecortin (DCX) (Fig. 1) and beta-III tubulin (TuJ1). Some putative immature neurons also expressed polysialylated neural cell adhesion molecule (PSA-NCAM), which is present in migratory cells. They also had ultrastructural features of immature migrating neurons (Supp. Fig. 2) similar to neuroblasts described in rodent SVZ[12]. Progressively, between 6 to 18 months of age, the SVZ is depleted of this dense network of putative migratory neurons and adopts the characteristic adult structure with an astrocyte ribbon and hypocellular gap layer. The emergence of the gap layer coincides with the decline in DCX(+) immature neurons (25-fold during the first 6 months; *n*=16, ages 0–17 years; Fig. 1), and proliferation, suggesting that human SVZ neurogenesis decreases drastically during the first 6 months of life. Only a small number of proliferating cells were present in adolescents and adults. Expression of the proliferation marker Ki67 was not associated with pyknotic nuclei, although we cannot exclude that some Ki67(+) nuclei correspond to apoptotic cells induced by ischemia[13]. We also identified a subpopulation of epidermal growth factor receptor (EGFR)-positive cells, a marker associated with early progenitors including neural stem cells[14] and transit-amplifying cells in mice[15], which similarly diminished with time (Supp. Fig. 3). A subset of EGFR(+) cells expressed Ki67, while others co-localized with DCX or PSA-NCAM, potentially representing transitional stages from transit-amplifying cells to immature neurons. Whole-mount, *en face*, preparations of the SVZ also confirmed massive numbers of tangentially-oriented DCX(+) chains within the gap layer at 1 week and 2 months of life. In stark contrast, cells with the morphology and marker expression of immature migratory neurons were extremely rare in adults (Supp. Fig. 4).

Our results suggest that robust streams of tangentially migrating immature neurons initially populate the postnatal human gap layer; these pathways become depleted between 6–18 months and this region transitions into a hypocellular gap. Previous work has also demonstrated a similarly sharp decline in the human SVZ's EGFR and PSA-NCAM immunoreactivity during the first year of life[17]. Within the SVZ, the decline of migratory immature neurons appears first along the posterior third of the lateral ventricle and then progresses in a posterior-to-anterior trajectory towards the ventral tip (data not shown). After 18 months, Ki67(+) proliferative activity and the number of DCX(+) immature neurons assume trace levels seen in adults, leaving behind the gap layer characteristic of the adult human SVZ[7].

We next investigated whether proliferation and the presence of putatively migrating, immature neurons in the SVZ were associated with an active RMS. Using autopsied material (*n=6*) (ages 1 day; 1 week; 1, 3, and 6 months), serial sagittal and coronal reconstruction of the ventral forebrain revealed an uninterrupted column of cells that connected the ventral tip of the SVZ to the olfactory peduncle (Fig. 2). The descending/proximal limb of the pediatric RMS contained cells organized as chains – large collections of elongated immature neurons expressing DCX and surrounded by glial cells and processes[1,4,18,19] (Fig. 2) – or as broad streams of individual cells. A subpopulation of these DCX(+) cells expressed PSA-NCAM. Conversely, analysis of tissue from older children (*n*=7; 2, 3, 7, 16, 17 years) failed to reveal chains of migrating cells or evidence of an active RMS. However, individual or pairs of elongated DCX(+)PSA-NCAM(+) putative migratory neurons were occasionally noted in late childhood specimens (*n*=2; 3 and 7 years) adults (*n*=5, ages 30, 41, 61, 74, 84 years). These observations indicate that, while the infant brain contains a robust RMS with massive chain migration, such activity is reduced dramatically in older children and adults[7]. Although, our data do not rule out that rare immature neurons may sporadically migrate within the SVZ and RMS at later stages[7,9], these findings do not support the previous finding of robust proliferation and abundant migration within the adult human SVZ[8].

The distal limb of the RMS delivers SVZ neuronal progeny to the human olfactory peduncle, and then to the olfactory tract (OT) and OB. Serial cross-sections of the OT (*n*=6; 1 day; 1 week; 5, 6, and 8 months) revealed clusters of DCX(+)PSA-NCAM(+) immature neurons within the V-shaped central core (Fig. 3). Electron microscopy analysis of the 6-month OT (*n*=3) confirmed ultrastructural features of migrating immature neurons within the core. Cross-sections of the proximal OT core (5mm anterior to the olfactory peduncle) at 8 months contained 234 ± 26 total cells and 173 ± 24 DCX(+) cells per section, respectively, while the distal OT core (5mm posterior to the OB) contained 216 ± 20 total cells and 115 ± 14 DCX(+) cells. In contrast, DCX(+) neurons were not detected in older OT specimens (*n*=3; 18 months, 7 and 13 years) (Fig. 3). These data further support that an active RMS exists in early childhood, but is greatly reduced after 18 months of age.

Although it has been suggested that an open olfactory ventricle persists into adult life[8], we found no evidence of a ventricular extension in the OT at any of the ages studied, consistent with previous data indicating that the olfactory ventricle fuses before birth[7,9,20]. Along the proximal limb of the RMS, we observed ependymal islets, but no evidence of a continuous open ventricle. These displaced and discontinuous islets were lined by multiciliated cuboidal cells expressing the ciliary marker acetylated-tubulin (Supp. Fig. 5). In all studied specimens (*n*=23), the anterior horn of the lateral ventricle was open, but no continuous, ependymal-lined lumen extending into the RMS or OT was observed. Thus, we infer that the human OT serves as a conduit for neuronal chain-migration to the OB, but these chains of migratory cells are only evident in infants and occur in the absence of a ventricular extension.

In tracing the ependymal islets of the pediatric human RMS with serial coronal reconstructions ($n = 3$), we noted a decrease in caliber of the RMS from the proximal to distal limb (Fig. 4). Based on quantification of DAPI nuclear staining, the proximal limb of the RMS contained 548 ± 66 total cells/cross-section and 485 ± 58 DCX(+) immature neurons/cross-section. In the distal limb, however, there were 228 ± 24 total cells/cross-section and 189 ± 17 DCX(+) immature neurons/cross-section, equating to a 58% decline in total cells and a 61% decline in immature neurons. The decreasing caliber of the RMS could be due to cell death, increased migratory speed, or immature migratory neurons taking alternative paths. Terminal deoxynucleotidyl transferase dUTP nick end labeled (TUNEL)-positive cells were present in the proximal and distal RMS, raising the possibility that apoptosis could contribute to this decline. However, serial coronal reconstruction of the frontal lobe also unexpectedly revealed an additional migratory stream of DCX(+) cells branching off the proximal limb of the RMS and ending in the ventro-medial pre-frontal cortex (VMPFC) (Fig. 4). This medial migratory stream (MMS) was observed in human specimens ages 4–6 months but not 8–18 months. Similar to the RMS, the MMS contains large clusters of DCX(+) and PSA-NCAM(+) cells with elongated morphologies, some adjacent to discontinuous ependymal islets (Supp. Fig. 5). Early timepoints (<1 month) also revealed a more diffuse pattern of medially-oriented migratory neurons emanating from the proximal limb of the primary RMS (Supp. Fig. 6). Interestingly, cells expressing DCX, PSA-NCAM, and the interneuron markers Calretinin (CalR) and Tyrosine Hydroxylase (TH), were observed not only within this MMS, but also within a restricted subregion of the VMPFC (Fig. 4). In contrast, very few DCX(+), PSA-NCAM(+), CalR(+), and TH(+) cells were evident in adjacent areas of prefrontal cortex. Although it remains possible that alterations in immunoreactivity allow progeny to escape into adjacent regions undetected, these observations suggest that the MMS diverts immature SVZ neurons to target the VMPFC.

A comparable MMS has not been reported in other vertebrates. We analyzed serial sections of mouse brains at P4, P8, P16 and P20 and did not detect a MMS (Supp. Fig. 7). However, some individual DCX positive cells were observed migrating ventrally and laterally in juvenile brain studied that might target homologous brain regions. In rodents and non-human primates, migratory neurons can also escape the SVZ along a sagittal plane to reach the Islands of Calleja[21,22].

Our study indicates that the region of the SVZ around the anterior lateral ventricles in the infant human brain is highly active, producing many tangentially-migrating immature neurons. Based on the presence of an RMS containing chains of immature neurons, we infer that at least some of these progeny are destined for the OB. Beyond 18 months of age, both proliferative activity and cells expressing markers of immature neurons are largely depleted, coinciding with the appearance of a hypocellular gap in the postnatal human SVZ. Thus, this layer of the SVZ initially serves as a thoroughfare for immature neurons. Surprisingly, pediatric human SVZ neurogenesis also appears to serve regions other than the OB, as evidenced by medially-escaping immature neurons near the RMS. These groups of cells form a unique MMS targeting a subregion of the human prefrontal cortex.

Previous work has suggested that postnatal neurogenesis may be important for learning and memory[23,24] and that induction of plasticity may be closely linked to the timing of neuronal maturation[25–27]. We speculate that the MMS, and other potential escape pathways from the SVZ, could supply interneurons to regions of the developing human brain as a mechanism of delayed postnatal plasticity. While the function of this recipient cortical domain, the VMPFC, is unknown in children, this region in the adult human brain is activated during specific cognitive tasks[28,29], including spatial conceptualization and the emotional processing of visual cues. Interestingly, the VMPFC is also focally inactivated in patients with advanced Alzheimer’s disease[30]. Beyond its functional implications, this developmental study of the human SVZ suggests a major period of neurogenesis and neuronal migration that extends well into postnatal life, but is largely limited to early childhood. This may hold important implications for our understanding of neonatal neurological diseases, including germinal matrix hemorrhages and perinatal hypoxic-ischemic injuries, each potentially altering SVZ neurogenesis and its apparent downstream cortical targets at formative stages of human development. Perhaps most importantly, the detection of a new migratory route for immature neurons within the infant human brain also highlights mechanisms through which increased regional complexity may be achieved during brain evolution.

Methods Summary

Human Specimens

Neurosurgical excisions of normal SVZ occurred as part of the planned margin of resection surrounding a periventricular lesion (Supplementary Table 1). Intraoperative specimens were histologically normal with no evidence of dysplasia, and assessments were independently confirmed by an independent neuropathologist. For pathological specimens, autopsied brains were cut coronally at the mammillary bodies and immersed in 4% paraformaldehyde (PFA) for 1–2 weeks, and then stored in 0.1M PBS.

Rodent Specimens

Postnatal mice at the specified ages were transcardially perfused with 0.9% saline and 4% PFA, and dissected brains were postfixed for 30 minutes in 4% PFA before vibratome sectioning. 100 micron floating sections were stained and imaged using the tile scanning and 3D projection modules on a Leica SP5 confocal microscope.

Immunohistochemistry

Tissue sections were incubated with primary antibodies diluted overnight at 4°C. Sections were then incubated for 2.5hrs in secondary antibodies and then incubated in streptavidin-horseradish peroxidase for 30’. Antigen retrieval with Proteinase K (10 ug/mL), or 0.01M Citrate buffer at 95°C was employed when necessary.

Whole-Mount Dissection

Specimens were fixed in 4% PFA for 3 days, then rinsed in 0.1M PBS. The anterior horn of the lateral ventricles is excised (3 mm squares) and rinsed. Tissue specimens were incubated in primary antibodies diluted in blocking solution for 2 nights. This step is repeated for secondary antibodies incubation. The ventricular face of tissue specimens is microdissected and collected at 200–300 μm thickness and mounted.

Electron Microscopy

Specimens fixed in 2% glutaraldehyde and 2% paraformaldehyde were cut into 200-mm sections on a vibratome. Sections were post-fixed in 2% osmium, rinsed, dehydrated and embedded in Araldite (Durcupan, Fluka). To identify individual cell types, ultrathin (0.05-mm) sections were cut with a diamond knife, stained with lead citrate and examined under a Jeol 100CX electron microscope.

Methods

Human Specimens

Neurosurgical excisions of normal SVZ occurred as part of the planned margin of resection surrounding a periventricular lesion (Supplementary Table 1). We recorded the anatomical origin of each intraoperative specimen with intraoperative neuronavigation. Intraoperative specimens were histologically normal with no evidence of dysplasia, and assessments were independently confirmed by an independent neuropathologist.

For pathological specimens, autopsied brains were cut coronally at the level of the mammillary bodies and immersed in 4% paraformaldehyde (PFA) for 1–2 weeks, and then stored in 0.1M PBS. The brains are then cut into 1 cm plates along the coronal, axial, or sagittal plane. The anterior horn of the lateral ventricle and the ventral medial aspect, which includes gyrus rectus and olfactory tract, of the frontal cortex are excised. Autopsy specimens were obtained within 12 h of death from all individuals. All causes of death were non-neurological in origin and all patients had no evidence of intracranial disease. All specimens were collected with informed consent and in accordance with the University of California San Francisco Committee on Human Research (IRB# H11170-19113).

Rodent Specimens

Postnatal mice at the specified ages were transcardially perfused with 0.9% saline and 4% PFA, and dissected brains were postfixed for 30 minutes in 4% PFA before vibratome sectioning. 100 micron floating sections were stained with rabbit anti-doublecortin (Cell Signaling), mouse anti-PSA-NCAM (Millipore), and DAPI (Sigma), mounted on Superfrost Plus slides, and imaged using the tile scanning and 3D projection modules on a Leica SP5 confocal microscope. Composite images were assembled from individual 10X fields using Adobe Photoshop. All experiments were approved by the UCSF Institutional Animal Care and Use Committee (Approval #AN077716).

Immunohistochemistry

All fixed specimens were rinsed in 0.1M PBS and then cut on a vibratome (50 μm), or cryoprotected in 30% sucrose and then cut on a cryostat (30 μm). Tissue sections were incubated with primary antibodies diluted in TNB blocking solution (0.1M Tris-HCl, pH 7.5, 0.15M NaCl, 0.5% blocking reagent from PerkinElmer) overnight at 4°C. Sections were then incubated for 2.5hrs in secondary antibodies diluted in TNB. Sections were then incubated in streptavidin-horse radish peroxidase for 30' in TNB, which catalyzes subsequent fluorescent conversion of tyramide substrates (all from PerkinElmer). Antigen retrieval with Proteinase K (10 ug/mL), or 0.01M Citrate buffer at 95°C was employed when necessary.

The following antibodies were used in this study: GFAP (Chemicon), Vimentin (Sigma), Doublecortin (Chemicon), TuJ1 (Covance), PSA-NCAM (Genbiosys), Ki67 (DAKO), Calretinin (Chemicon), Calbindin (Chemicon), Tyrosine Hydroxylase (Chemicon), and EGFR (Upstate Biotechnology).

Whole-Mount Dissection

Specimens were fixed in 4% PFA for 3 days, then rinsed in 0.1M PBS. The anterior horn of the lateral ventricles is excised (3 mm squares) and rinsed in 0.1% PBS-Triton X-100. Tissue specimens were incubated in primary antibodies diluted in blocking solution (10% normal goat serum, 2% TritonX-100, 0.1M PBS) for 2 nights. This step is repeated for secondary antibodies incubation. DAPI was used (1:500) for counterstaining, and Aqua Polymount (Polysciences) for mounting. The ventricular face of tissue specimens is microdissected and collected at 200–300 μm thickness and mounted.

In Situ Hybridization

Probes specific to human GFAP, doublecortin, and EGFR were generated by amplifying fragments from commercially available cDNA clones (Open Biosystems) or reverse-transcribed cDNA from human fetal brain total RNA (Clontech). Primer sequences for amplifying GFAP (Allen human Brain Atlas primer ID398603) and doublecortin (primer ID399287) were obtained from Allen Institute for Brain Science (http://www.brain-map.org/). Forward primer 5'-AGCTCTTCGGGGAGCAGCGA-3' and reverse primer 5'-TGCACGTGGCTTCGTCTCGG-3' were used for EGFR. Amplified fragments were subcloned into pCRII (Invitrogen) and RNA probes were made subsequently using DIG RNA labeling (Roche). Sections were cut at 14 μm, mounted on Superfrost Plus slides. The sections were pre-hybridized for 2 hours and hybridized with probes at 1:100 to 1:200 dilutions at 55°C overnight. After hybridization, slides were washed and incubated with anti-DIG antibody, and developed by BM purple substrate for 24 to 48 hours. Slides hybridization with GFAP and doublecortin RNA probes were subsequently immunostained with GFAP and doublecortin antibodies as previously described.

Electron Microscopy

Specimens fixed in 2% glutaraldehyde and 2% paraformaldehyde were cut into 200-mm sections on a vibratome. Sections were post-fixed in 2% osmium, rinsed, dehydrated and embedded in Araldite (Durcupan, Fluka). To study SVZ architecture, we cut serial 1-mm semithin sections and stained them with 1% toluidine blue. To identify individual cell types, ultrathin (0.05-mm) sections were cut with a diamond knife, stained with lead citrate and examined under a Jeol 100CX electron microscope.

Supplementary Material

Refer to Web version on PubMed Central for supplementary material.

Acknowledgements

The authors are grateful to Jeanelle Agudelo and Ricardo Romero for expert technical assistance and to Kenneth X. Probst for illustrations. N.S. was supported by an NIH F32 NRSA postdoctoral fellowship (NS 058180). R.I. was supported by fellowships from the Damon Runyon Cancer Research Foundation (DRG1935-07) and American Association for Cancer Research / National Brain Tumor Society. R.H. thanks the American Association for Cancer Research for support. This work was supported by grants from the NIH (NS 28478 and HD 32116 to AAB and NS 059893 to DHR), the Pediatric Brain Tumor Foundation, and by the John G. Bowes Research Fund. DHR is a Howard Hughes Medical Institute Investigator. AAB is the Heather and Melanie Muss Endowed Chair of Neurological Surgery at UCSF.

References

1. Kornack DR, Rakic P. The generation, migration, and differentiation of olfactory neurons in the adult primate brain. Proceedings of the National Academy of Sciences of the United States of America. 2001; 98:4752–4757. [PubMed: 11296302]
2. Blakemore WF, Jolly RD. The subependymal plate and associated ependyma in the dog. An ultrastructural study. Journal of neurocytology. 1972; 1:69–84. [PubMed: 4589051]
3. Perez-Martin M, et al. Ependymal explants from the lateral ventricle of the adult bovine brain: a model system for morphological and functional studies of the ependyma. Cell and tissue research. 2000; 300:11–19. [PubMed: 10805071]
4. Ponti G, Aimar P, Bonfanti L. Cellular composition and cytoarchitecture of the rabbit subventricular zone and its extensions in the forebrain. The Journal of comparative neurology. 2006; 498:491–507. [PubMed: 16874818]
5. Pencea V, Bingaman KD, Freedman LJ, Luskin MB. Neurogenesis in the subventricular zone and rostral migratory stream of the neonatal and adult primate forebrain. Experimental neurology. 2001; 172:1–16. [PubMed: 11681836]
6. Young KM, Fogarty M, Kessaris N, Richardson WD. Subventricular zone stem cells are heterogeneous with respect to their embryonic origins and neurogenic fates in the adult olfactory bulb. J Neurosci. 2007; 27:8286–8296. [PubMed: 17670975]
7. Sanai N, et al. Unique astrocyte ribbon in adult human brain contains neural stem cells but lacks chain migration. Nature. 2004; 427:740–744. [PubMed: 14973487]
8. Curtis MA, et al. Human neuroblasts migrate to the olfactory bulb via a lateral ventricular extension. Science (New York, N.Y. 2007; 315:1243–1249.
9. Sanai N, Berger MS, Garcia-Verdugo JM, Alvarez-Buylla A. Comment on "Human neuroblasts migrate to the olfactory bulb via a lateral ventricular extension". Science (New York, N.Y. 2007; 318:393. author reply 393.
10. Guerrero-Cazares H, et al. Cytoarchitecture of the lateral ganglionic eminence and rostral extension of the lateral ventricle in the human fetal brain. The Journal of comparative neurology. 2011; 519:1165–1180. [PubMed: 21344407]
11. Zecevic N. Specific characteristic of radial glia in the human fetal telencephalon. Glia. 2004; 48:27–35. [PubMed: 15326612]
12. Wichterle H, Garcia-Verdugo JM, Alvarez-Buylla A. Direct evidence for homotypic, glia-independent neuronal migration. Neuron. 1997; 18:779–791. [PubMed: 9182802]

13. Kuan CY, et al. Hypoxia-ischemia induces DNA synthesis without cell proliferation in dying neurons in adult rodent brain. The Journal of neuroscience : the official journal of the Society for Neuroscience. 2004; 24:10763–10772. [PubMed: 15564594]
14. Pastrana E, Cheng LC, Doetsch F. Simultaneous prospective purification of adult subventricular zone neural stem cells and their progeny. Proceedings of the National Academy of Sciences of the United States of America. 2009; 106:6387–6392. [PubMed: 19332781]
15. Doetsch F, Petreanu L, Caille I, Garcia-Verdugo JM, Alvarez-Buylla A. EGF converts transit-amplifying neurogenic precursors in the adult brain into multipotent stem cells. Neuron. 2002; 36:1021–1034. [PubMed: 12495619]
16. Mirzadeh Z, Merkle FT, Soriano-Navarro M, Garcia-Verdugo JM, Alvarez-Buylla A. Neural stem cells confer unique pinwheel architecture to the ventricular surface in neurogenic regions of the adult brain. Cell stem cell. 2008; 3:265–278. [PubMed: 18786414]
17. Weickert CS, et al. Localization of epidermal growth factor receptors and putative neuroblasts in human subependymal zone. The Journal of comparative neurology. 2000; 423:359–372. [PubMed: 10870078]
18. Lois C, Alvarez-Buylla A. Long-distance neuronal migration in the adult mammalian brain. Science (New York, N.Y. 1994; 264:1145–1148.
19. Rodriguez-Perez LM, Perez-Martin M, Jimenez AJ, Fernandez-Llebrez P. Immunocytochemical characterisation of the wall of the bovine lateral ventricle. Cell and tissue research. 2003; 314:325–335. [PubMed: 14513354]
20. Humphrey TJ. The development of the olfactory and accessory olfactory formation in human embryos and fetuses. Journal of Comparative Neurology. 1940; 73:431–468.
21. Bedard A, Levesque M, Bernier PJ, Parent A. The rostral migratory stream in adult squirrel monkeys: contribution of new neurons to the olfactory tubercle and involvement of the antiapoptotic protein Bcl-2. Eur J Neurosci. 2002; 16:1917–1924. [PubMed: 12453055]
22. Meyer G, Gonzalez-Hernandez T, Carrillo-Padilla F, Ferres-Torres R. Aggregations of granule cells in the basal forebrain (islands of Calleja): Golgi and cytoarchitectonic study in different mammals, including man. The Journal of comparative neurology. 1989; 284:405–428. [PubMed: 2474005]
23. Zhao C, Deng W, Gage FH. Mechanisms and functional implications of adult neurogenesis. Cell. 2008; 132:645–660. [PubMed: 18295581]
24. Nottebohm F. The road we travelled: discovery, choreography, and significance of brain replaceable neurons. Ann N Y Acad Sci. 2004; 1016:628–658. [PubMed: 15313798]
25. Bovetti S, Veyrac A, Peretto P, Fasolo A, De Marchis S. Olfactory enrichment influences adult neurogenesis modulating GAD67 and plasticity-related molecules expression in newborn cells of the olfactory bulb. PLoS One. 2009; 4:e6359. [PubMed: 19626121]
26. Nissant A, Bardy C, Katagiri H, Murray K, Lledo PM. Adult neurogenesis promotes synaptic plasticity in the olfactory bulb. Nat Neurosci. 2009; 12:728–730. [PubMed: 19412168]
27. Southwell DG, Froemke RC, Alvarez-Buylla A, Stryker MP, Gandhi SP. Cortical plasticity induced by inhibitory neuron transplantation. Science (New York, N.Y. 2010; 327:1145–1148.
28. Longe O, Senior C, Rippon G. The lateral and ventromedial prefrontal cortex work as a dynamic integrated system: evidence from FMRI connectivity analysis. Journal of cognitive neuroscience. 2009; 21:141–154. [PubMed: 18476765]
29. Szatkowska I, Szymanska O, Grabowska A. The role of the human ventromedial prefrontal cortex in memory for contextual information. Neuroscience letters. 2004; 364:71–75. [PubMed: 15196680]
30. Herholz K, et al. Discrimination between Alzheimer dementia and controls by automated analysis of multicenter FDG PET. NeuroImage. 2002; 17:302–316. [PubMed: 12482085]

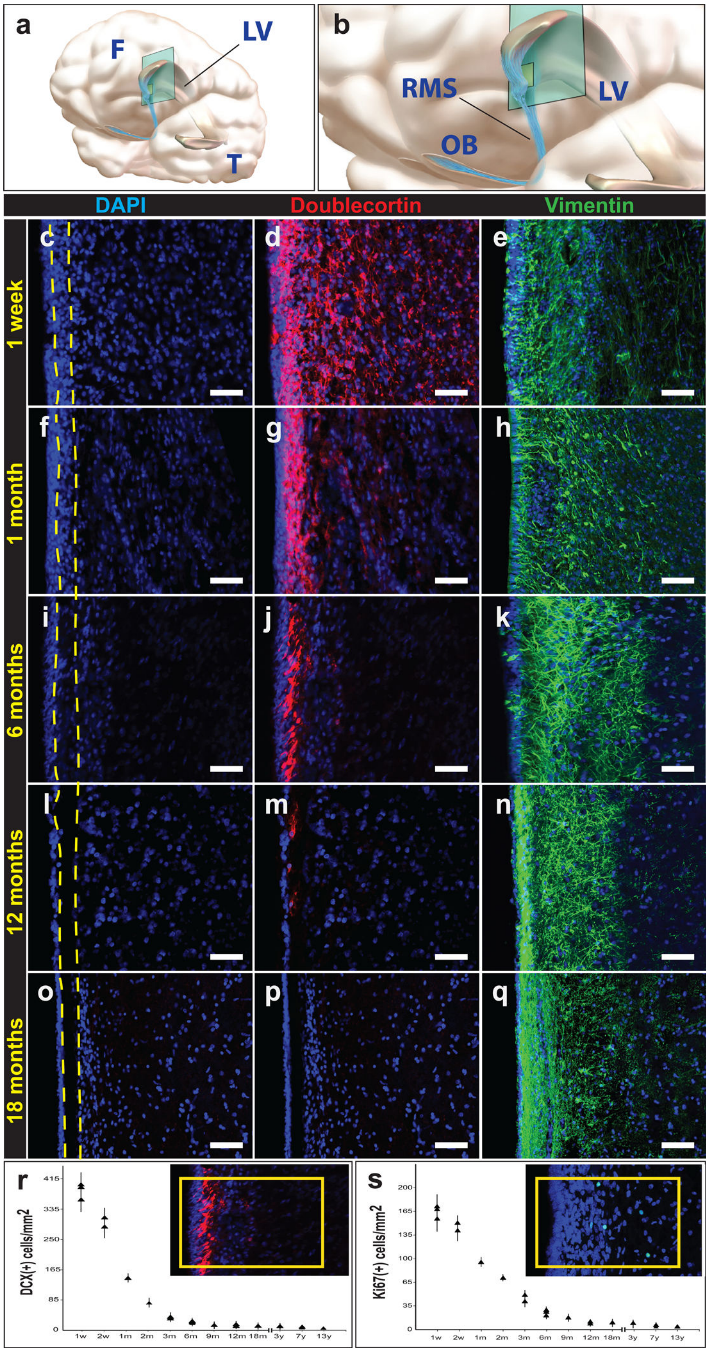

Figure 1. Cytoarchitectural development of the human SVZ during the first 18 months of life

(a, b) Illustrations localizing the horizontal 30μm sections of the anterior ventral SVZ labeled with nuclear marker DAPI (c, f, i, l, o), the immature migrating neuronal marker Doublecortin (DCX) (d, g, j, m, p) and the immature glial marker Vimentin (e, h, k, n, q). F=frontal lobe, T=temporal lobe, LV=lateral ventricle, RMS=rostral migratory stream, OB=olfactory bulb. Large numbers of DCX(+) immature migrating neurons populate the region that develops into the human gap layer (yellow dotted lines). In the first few months of life, radial glia-like Vimentin(+) cells are seen to populate the ventricular lining (e, h), and at 12 months onward, a dense network of Vimentin(+) processes fill the gap area (n, q). DCX and DAPI are co-labeled in the same section (first and second columns), while Vimentin staining is from adjacent sections (third column). (r) DCX(+) immature neurons within the anterior ventral SVZ were quantified in ten 20x fields per section, ten sections per specimen, and 1–3 specimens per timepoint. Each data point represents the mean +/− SD of a single specimen at the designated age (w = week, m = month, y = year). Inset demonstrates the field of quantification (yellow box) for each of the 10 horizontal sections per specimen. (s) Proliferating Ki67(+) subependymal cells were similarly quantified along the anterior ventral human SVZ. Taken together, these data demonstrate, during the first 18 months of life, a sharp decline in proliferating cells and immature migrating neurons coinciding with emergence of the human SVZ gap layer. Scale bars = 30μm.

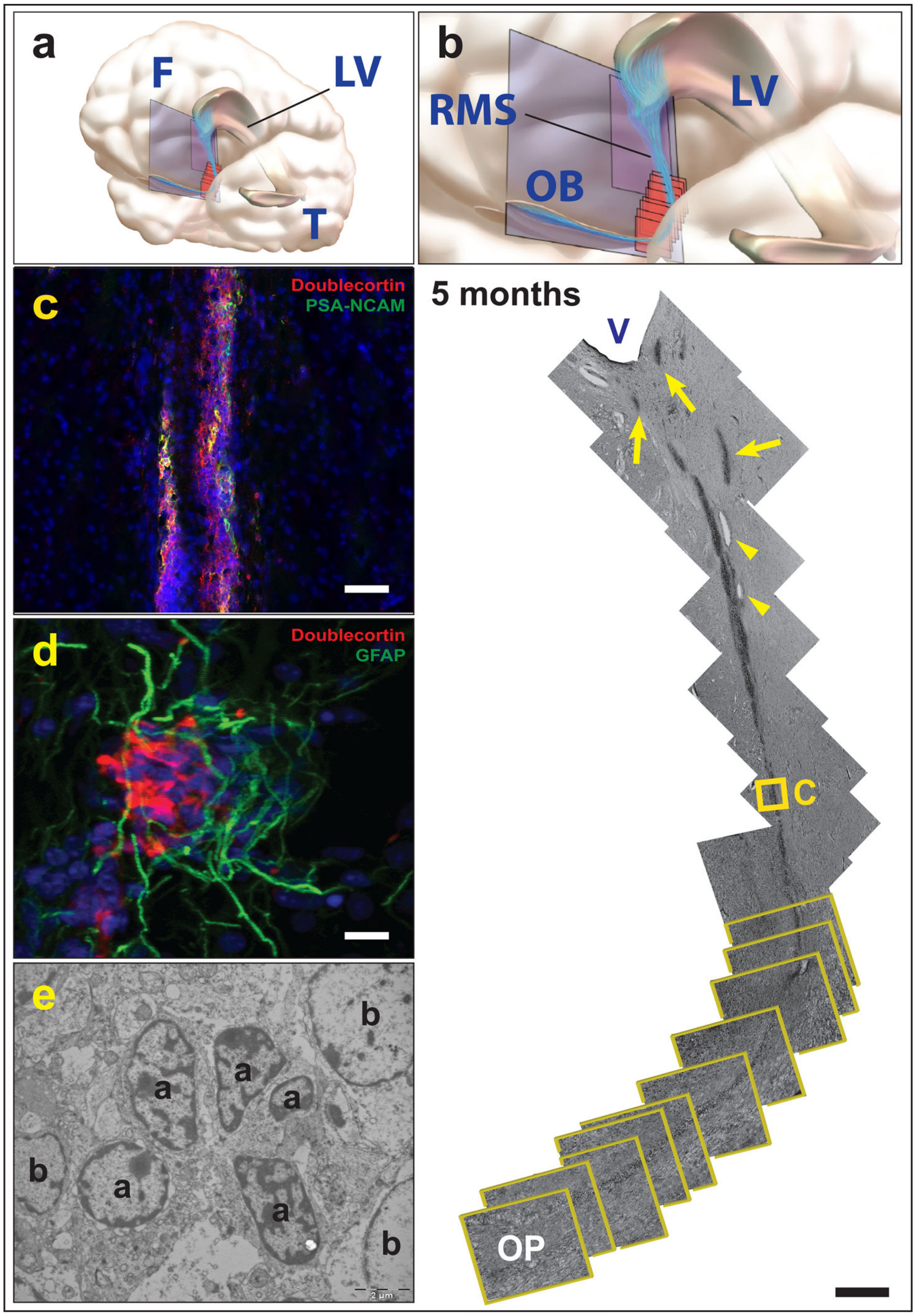

Figure 2. The infant human rostral migratory stream connects the subventricular zone to the olfactory peduncle

Reconstruction of serial sagittal sections of a hematoxylin-stained RMS from inferior lateral ventricle (V) to olfactory peduncle (OP) of an infant specimen (5 months of age). The subventricular source of the proximal RMS shows multiple tributaries of cells (yellow arrows) that appear to coalesce forming the descending (proximal) limb of the RMS. There is no evidence of a continuous ventricular system, but isolated ependymal islets (yellow arrowheads) are observed along the RMS. The distal limb of the RMS moves laterally, out of the sagittal plane of sectioning, as indicated by the yellow section frames. (a, b)

Illustrations indicating the anatomic site, plane, and orientation of tissue sectioning, as described above. F=frontal lobe, T=temporal lobe, LV=lateral ventricle, RMS=rostral migratory stream, OB=olfactory bulb. (c) The yellow rectangle indicated along the proximal limb of the RMS demonstrates clusters of DCX(+)PSA-NCAM(+) immature neurons at higher magnification. (d) Individual DCX(+) neuronal chains, seen here in the ventral tip of the anterior horn of a 1-week specimen, are typically embedded in a matrix of GFAP(+) glial processes and often migrate along blood vessels (see Supp. Fig 4d). (e) Ultrastructural analysis of a neuronal chain cross-section identifies immature neurons (type A cells, labeled 'a') surrounded by glia (type B cells, labeled 'b'). Scale bars = 500mm (reconstruction), 50μm (c), and 10μm (d).

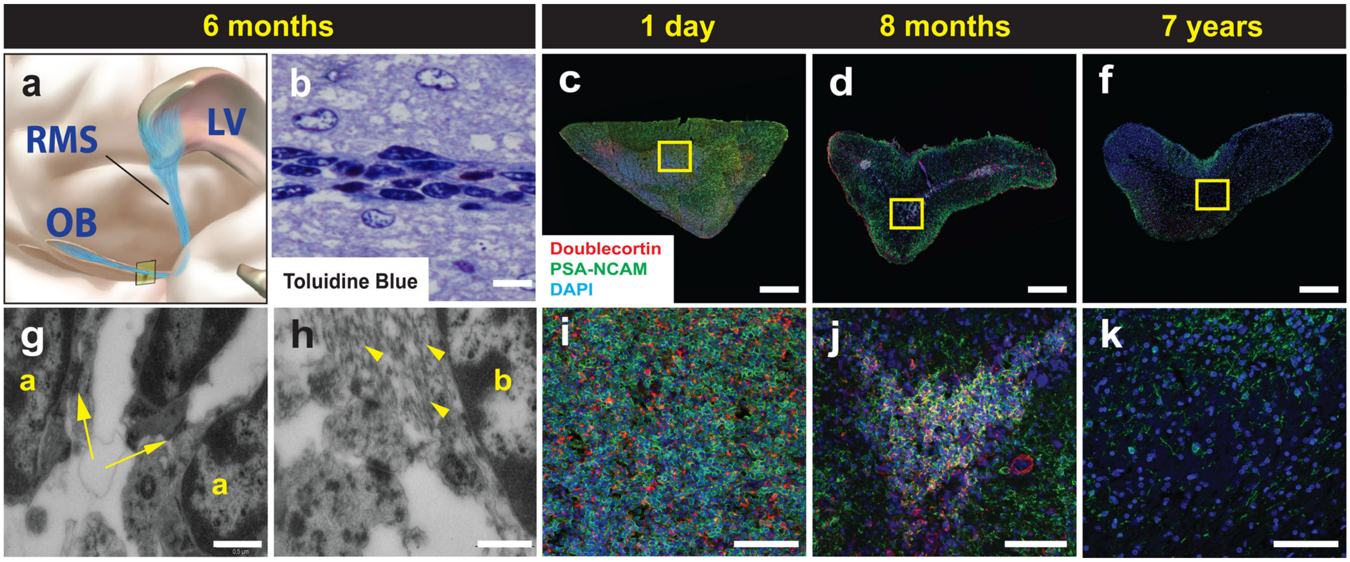

Figure 3. Postnatal development and decline of the RMS in the human olfactory tract (OT)

(a) Illustration localizes the anatomical sites for cross-sectional reconstructions of the proximal human OT at (c, i) 1 day, (d, j) 8 months, and (f, k) 7 years. LV=lateral ventricle, RMS=rostral migratory stream, OB=olfactory bulb. High-magnification fields (i, j, k) demonstrate progressive loss of DCX(+)PSA-NCAM(+) immature neurons in the OT. An active RMS is evident at birth and 8 months of age, with many DCX(+)PSA-NCAM(+) cells. By 7 years, however, chains of migrating cells are not observed and DCX(+) cells are rare. (b) Toluidine blue staining of a longitudinal semithin (6μm) section from a 6-month OT demonstrates a central chain of darkened immature neurons surrounded by a matrix of lighter-colored astrocytes. (g) Electron microscopy also demonstrates clusters of type A cells (labeled ‘a’) enmeshed with type B cells within the OT core, including intercellular junctions (yellow arrows) between immature neurons characteristic of chain migration and (h) intermediate filaments (yellow arrowheads) within surrounding Type B cells (labeled ‘b’). Scale bars = 500μm (c, d, f); 75μm (i, j, k); 10μm (b); and 0.5μm (g, h).

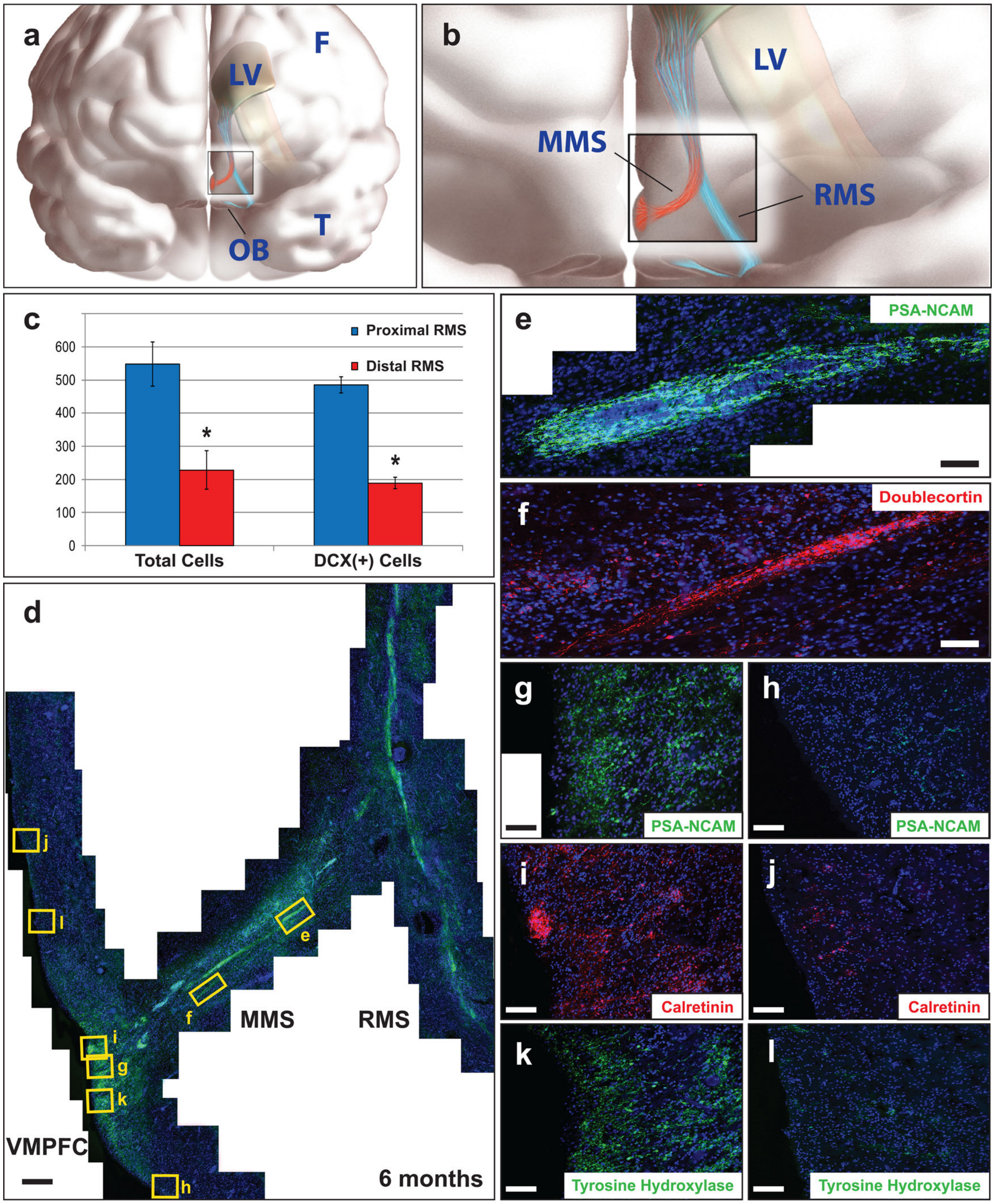

Figure 4. A medial migratory stream (MMS) of immature neurons branches from the proximal rostral migratory stream (RMS) in the infant human brain to supply the ventromedial prefrontal cortex (VMPFC)

(a, b) Illustrations demonstrate the anatomical site of the RMS (blue) and MMS (red). F=Frontal lobe, T=Temporal lobe, LV=lateral ventricle, OB=olfactory bulb. (c) Using cross-sections of the proximal and distal RMS, quantifications of the total number of cells and total number of DCX(+) cells per cross section indicated a significant reduction from proximal to distal RMS. Asterisks indicate $p<0.05$. (d) Coronal reconstruction of a 6-month specimen reveals a PSA-NCAM(+) medial migratory stream diverging from the RMS to reach the VMPFC. (e) Within this medial migratory stream, chains of PSA-NCAM(+) cells co-express (f) the immature neuronal marker DCX. (g, i, k) Dense clusters of PSA-NCAM(+), Calretinin(+), and Tyrosine Hydroxylase(+) cells are specifically observed within a subregion of the VMPFC, but not at adjacent cortical sites (h, j, l) superior or inferior to this subregion. Scale bars = 150μm (d), 20μm (e–l).